Rheology-Processing-Property Relationships in Tubular Blown Film Extrusion. I. High-Pressure Low-Density Polyethylene

CHANG DAE HAN and TAE HOON KWACK, *Department of Chemical Engineering, Polytechnic Institute of New York, Brooklyn, New York 11201*

Synopsis

Three different grades of high-pressure low-density polyethylene resin were used to establish relationships between tubular film blowability and the molecular parameters, namely, the molecular weight distribution (MWD) and the degree of long-chain branching (LCB), and also between the processing conditions and the mechanical properties of the tubular blown films produced. For the study, both the shearing and elongational flow properties of the resins were determined. During the tubular film blowing experiment we measured the freeze-line position, the tubular bubble diameter, the takeup speed, the axial tension, the pressure inside the tubular bubble, and the mass flow rate of the resin. The thickness of the tubular blown films was measured from the samples collected. In order to determine the tubular film blowability, we measured the maximum takeup speed at which the tubular blown bubble broke, for various blowup ratios. The measurements described above permitted us to calculate the tensile stresses at the freeze line, in both the machine and transverse directions, and they were found to be correlatable to the processing conditions employed. It has been found that the tubular film blowability is increased as the resin's MWD becomes narrower and the degree of LCB is less. It has been found further that a resin having lower elongational viscosity tends to give a greater draw-down ratio, indicating a better tubular film blowability. Finally, the tensile properties of the tubular blown films were found correlatable to the processing variables, namely, blowup and takeup ratios.

INTRODUCTION

Low-density polyethylene is a thermoplastic resin very widely used in the manufacture of film by the tubular film blowing process. Although numerous investigators[1–6] have reported the rheological behavior of low-density polyethylene (LDPE), very few have discussed any relationships between the rheological properties of the resin and its tubular film blowability, or between the molecular parameters and the tubular film blowability.

It is a well-recognized fact today that, due to the presence of long-chain branching in high-pressure low-density polyethylene (HP-LDPE), the molecular characterization of this type of resin is much more difficult and tedious than for linear polymers (e.g., high-density polyethylene, polypropylene). In recent years, some serious efforts[7–14] have been spent on developing experimental techniques for improving the accuracy of the determination of molecular parameters, especially the amount of long-chain branching (LCB), in HP-LDPE. Note that the accurate determination of these molecular parameters, that is, the molecular weights ($\overline{M}_n$, $\overline{M}_w$) and the amount of LCB, is essential to helping understand and correctly interpreting the resin's rheological behavior.

Journal of Applied Polymer Science, Vol. 28, 3399–3418 (1983)
 CCC 0021-8995/83/113399-20$03.00

Farber and Dealy[15] and Han and Park[16] experimentally studied the kinematics involved with tubular film blowing, and Han and co-workers[17–19] studied the sensitivity of the tubular film blowing characteristics of various thermoplastic resins to the rheological and processing variables. Maddams and Preedy[20–23] and Choi et al.[24] have also studied the development of crystalline orientation and the morphology of high-density polyethylene tubular blown films, and White and co-workers[25,26] have studied the development of orientation and mechanical properties of polystyrene tubular blown films.

The processability of a polymer is intimately related to its rheological behavior, which, in turn, depends on the molecular parameters, namely, molecular weight and its distribution, and the degree of long-chain branching. What makes the matter complicated is that, whereas the rheological behavior of a polymer is a direct response to molecular parameters, it also depends on many other factors. These include: (1) the types of flow field (i.e., kinematics); (2) the intensity of the rate of deformation; (3) temperature; (4) the deformation and thermal histories. Moreover, for a given polymer, one type of rheological response (e.g., shear viscosity) is not as sensitive to a slight change in molecular parameters as others (e.g., normal stress effects).

Furthermore, relatively little literature has been published dealing with the *processability* of polymers. It should be pointed out that any discussion about *processability* must refer to particular polymer processing operations. In this context, one may discuss, for instance, spinnability, injection (compression or transfer) moldability, tubular film blowability, thermoformability, foam extrudability, blow moldability, etc. Since polymer melt processing operations invariably involve fluid flow and heat transfer, and sometimes mass transfer and chemical reactions, any meaningful discussion of the processability of polymers cannot be done with rheological measurements alone. This is because, for instance, a polymer that has good extrudability may have poor injection moldability. This then raises a fundamental question about defining processability in reference to particular polymer processing operations.

From the processing point of view, two difficulties must be overcome in order to achieve a successful tubular film blowing operation. One is to avoid *bubble instability* and the other is to avoid *breakage* of the tubular blown bubble. The former gives rise to a nonuniform thickness of the films produced, and the latter limits the choice of takeup speed and blowup ratio, thus preventing one from producing thin-gauge films. Both processing difficulties have their origins in the molecular parameters and hence the rheological properties of polymers. However, it is generally believed that bubble instability is also closely related to the choice of processing conditions, whereas breakage of the tubular blown bubble (hereafter referred to as film blowability) is determined largely by the rheological behavior of the polymer being processed.

As part of our continuing effort to establish relationships between the rheological properties and the processability of polymeric materials, we have very recently embarked on a comprehensive research program for investigating the tubular film blowability of low-density polyethylene. Our study consists of two parts, the *first* dealing with high-pressure low-density polyethylene (HP-LDPE) and the *second* dealing with low-pressure low-density polyethylene (LD-LDPE). In this paper we shall present the results of the *first* part of our study.

TABLE I
Molecular Characterization Data for the Low-Density Polyethylene Resins Used

Resin	Density	Melt index	$\overline{M}_n$	$\overline{M}_w$	$\overline{M}_w/\overline{M}_n$	$\overline{M}_z$	$\overline{\lambda}_N$[a]
A	0.918	2.04	2.13×10^4	2.01×10^5	9.43	1.25×10^5	3.4
B	0.921	2.51	2.25×10^4	1.43×10^5	6.03	5.61×10^5	2.5
C	0.923	2.24	2.63×10^4	1.10×10^5	4.18	3.20×10^5	1.6

[a] $\overline{\lambda}_N$ represents the long-chain branching frequency, defined as the number-average number of branch point per 1000 carbon atoms.

EXPERIMENTAL

Materials. Long-chain branching low-density polyethylene is commonly referred to as high-pressure low-density polyethylene (HP-LDPE). Three different grades were used, the materials being supplied to us by Dr. George Foster at Union Carbide Corp. These resins were prepared in a commercial reactor specifically for the experimental research proposed by us. The molecular characterization of the resins was performed by Dr. George Foster himself. Table I gives information on the molecular weights, molecular weight distribution, and long-chain branching frequency, and Figure 1 gives the molecular weight distribution curves for the three resins. The methods employed for determining the molecular parameters given in Table I are described in a paper by Foster et al.[14]

Rheological measurement. The steady shearing flow properties were determined using a cone-and-plate rheometer (a Model R-16 Weissenberg rheo-

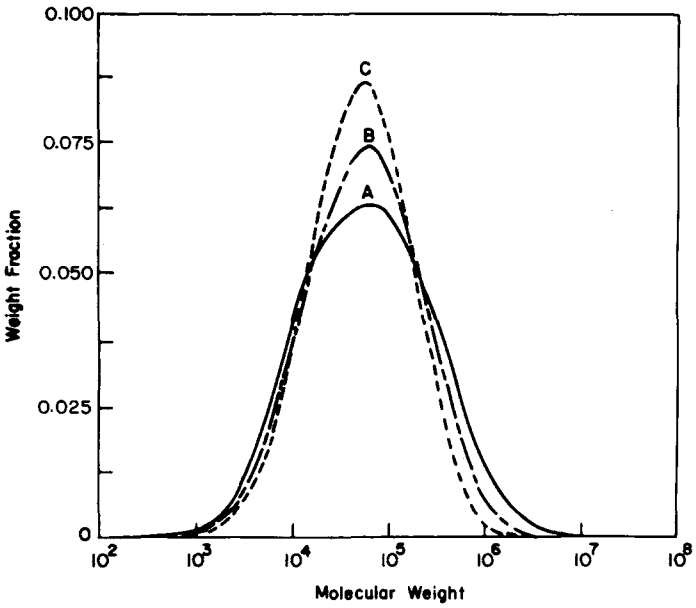

Fig. 1. Molecular weight distribution curves of the three long-chain branching low-density polyethylene resins investigated.

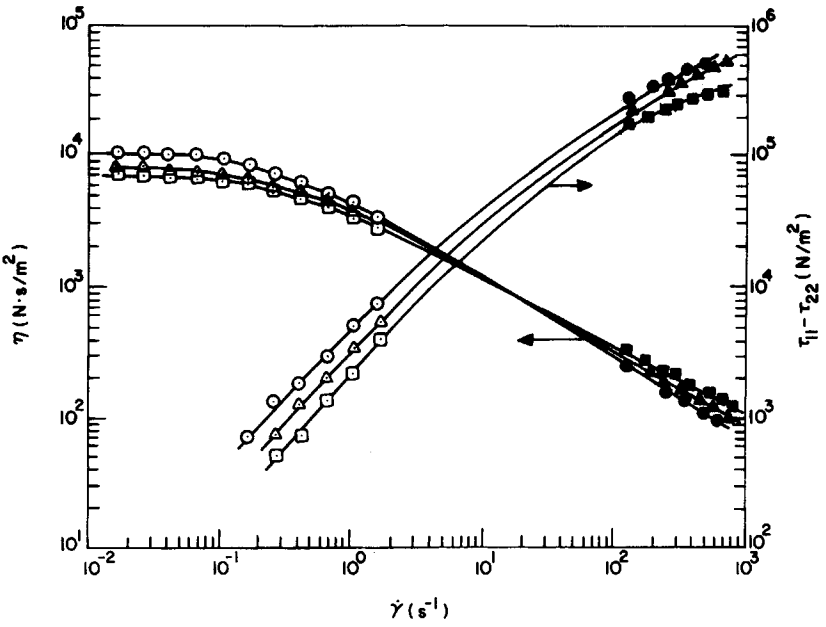

Fig. 2. η and $\tau_{11} - \tau_{22}$ vs. $\dot{\gamma}$ for the three LDPE resins investigated at 200°C: (⊙, ●) resin A; (△, ▲) resin B; (⊡, ■) resin C; (⊙, △, ⊡) data taken with a cone-and-plate rheometer; (●, ▲, ■) data taken with a slit/capillary rheometer.

goniometer) at *low* shear rates, and a slit/capillary rheometer at *high* shear rates. (A commercial version of the latter rheometer is available at Seiscor Division, Seismograph Service Corp., Tulsa, Okla.) The principles involved with these rheometers are well documented in the literature.[6] Figure 2 gives plots of shear viscosity η and first normal stress difference $\tau_{11} - \tau_{22}$ versus shear rate $\dot{\gamma}$ for the three resins employed, in which open symbols represent the data taken with a cone-and-plate rheometer and closed symbols represent the data taken with the slit/capillary rheometer.

The elongational viscosity was determined using the apparatus developed at the University of Tennessee. The details of the experimental procedure and the principles involved with data analysis are given in a paper by Ide and White.[27] Figures 3–5 give plots of elongational viscosity vs. time for the three resins employed, at various values of constant elongation rate. It is seen that, at an elongation rate of 0.01 s^{-1}, all three resins achieved steady state, but, at higher elongation rates, steady states were not achieved, except with resin C at an elongation rate of 0.1 s^{-1}.

Tubular film blowing experiment. The apparatus employed for the tubular film blowing experiment was, except for the extrusion die, essentially the same as that described in a previous paper by Han and Park.[16] In the present study, a new tubular die was fabricated (2.541 cm inner diameter and 2.698 cm outer diameter) and, also, a new cooling ring was employed. The molten polymer tube, upon exiting from the die, was cooled by an air stream distributed radially (i.e., pointed toward the outer surface of the bubble) by the cooling ring. In order to cool the air below room temperature, we first removed the moisture in the air by passing it through a long column packed with calcium silicate particles, and

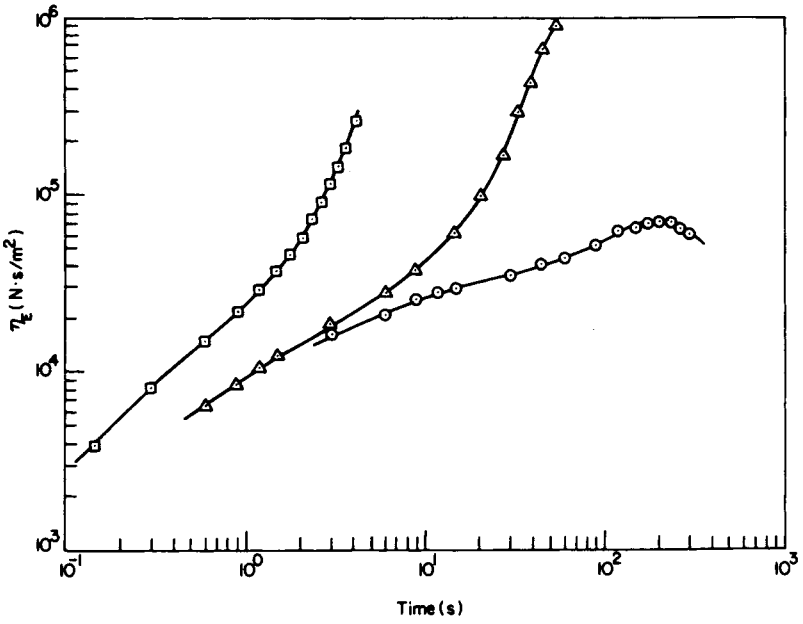

Fig. 3. Elongational viscosity vs. time for resin A (T = 180°C) at various values of constant elongation rate (s^{-1}): (⊙) 0.01; (△) 0.1; (⊡) 1.0.

then forced the dried air to flow through a long coil immersed in a refrigerating system, cooled by a Freon.

During the tubular film blowing experiment, the following variables were measured: (a) the tension, using a Bar Tensiometer (Tensitron Co.); (b) the air

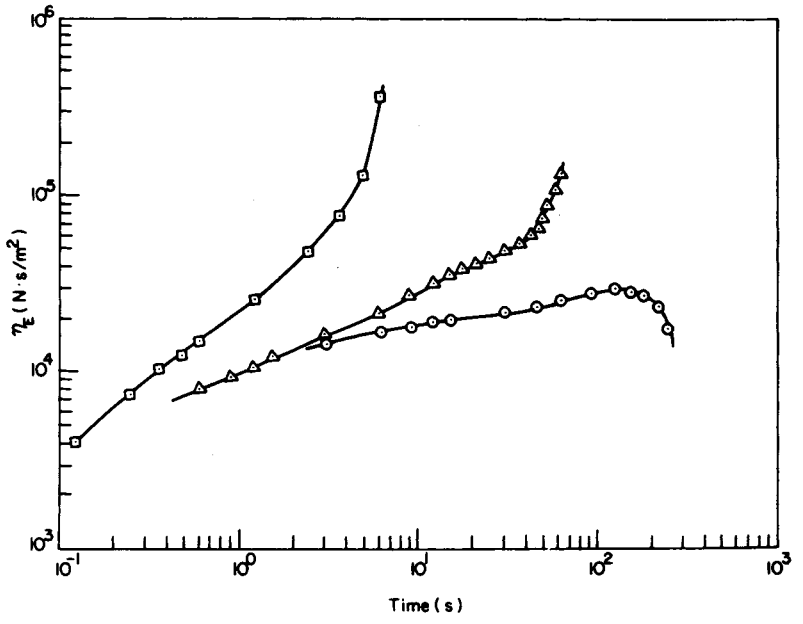

Fig. 4. Elongational viscosity vs. time for resin B (T = 180°C) at various values of constant elongation rate (s^{-1}): (⊙) 0.01; (△) 0.1; (⊡) 1.0.

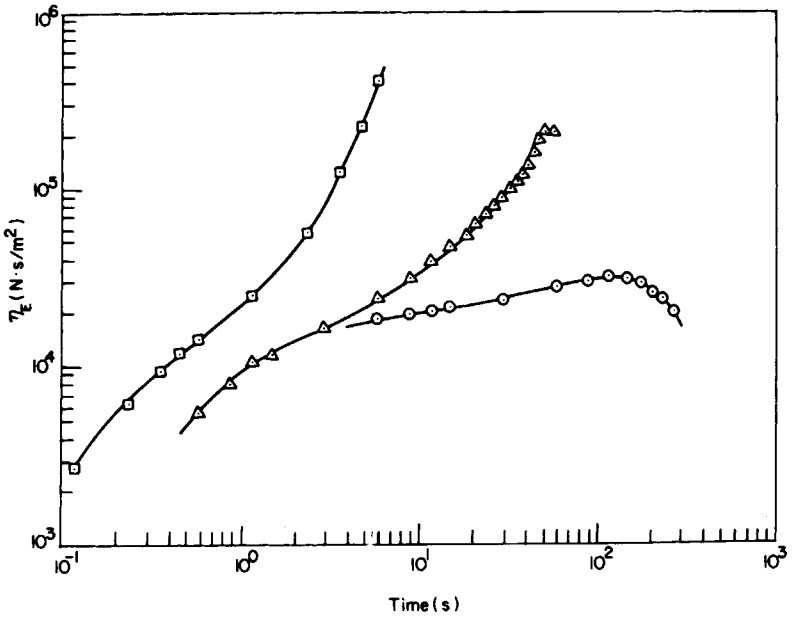

Fig. 5. Elongational viscosity vs. time for resin C (T = 180°C) at various values of constant elongation rate (s^{-1}): (⊙) 0.01; (▲) 0.1; (⊡) 1.0.

pressure inside the tubular bubble, using a water manometer; (c) the temperature and flow rate of the cooling air; (d) the mass flow rate of molten polymer (and hence the linear velocity of the melt at the die lip); (e) the melt temperature; (f) the diameter of the tubular bubble; (g) the position of the freeze line; (h) the thickness of the tubular blown film. Special attention was paid to determining the processing conditions at which the tubular bubble broke. For this, we slowly increased the takeup speed, while maintaining the blowup ratio constant, until the tubular bubble broke. We repeated the experiment at various blowup ratios. In each run, we recorded the tension and the position of the freezeline, and collected the film sample. Later, we measured the film thickness at a number of points along the machine direction of the samples collected. As will be discussed below, these measurements allowed us to calculate the tensile stresses in the film, in both the machine and transverse directions. The calculation of stresses has enabled us to correlate the tubular film blowing characteristics of the resins to their rheological properties, and to correlate the processing variables to the mechanical properties of the tubular blown films produced.

Tensile property measurement. Tensile properties of the film samples were determined at room temperature, using an Instron testing machine. Measurements were taken on several samples collected under identical processing conditions, and the average value was calculated.

Optical property measurement. Both gloss and haze measurements of the film samples were made, the former following the procedure described in ASTM D-2457-70 and the latter following the procedure described in ASTM D-1003-61.

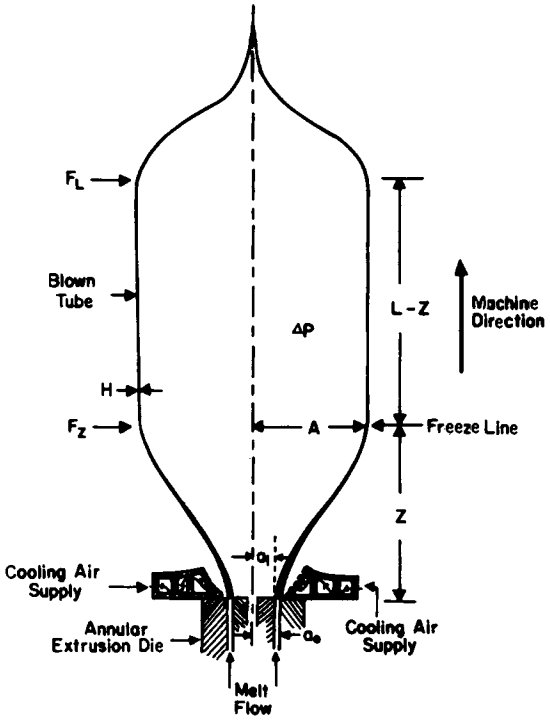

Fig. 6. Schematic describing the film blowing process.

DERIVATION OF WORKING EQUATIONS

In order to facilitate the discussion of our experimental results below, let us refer to the schematic given in Figure 6. We will derive in this section the working equations that describe the relationships between the processing variables and the rheological variables at the freeze line, as a molten tubular film is blown up and is carried away along the machine direction. Note that we will *not* be concerned with the region where the kinematics of biaxial stretching are involved (i.e., the region between the die exit and the freeze line). We are well aware of the fact that the stresses (hence the mechanical properties) in the film at the freeze line are dependent, among many factors, upon the melt extrusion temperature, the rate of cooling, and the development of crystalline orientation and morphology. However, because of the practical difficulty in incorporating the crystallization and orientation phenomena into the force balance equations at the freeze line, in the following derivation we will consider only the macroscopic force balance in the region between the freeze line and the position at which the axial tension is measured.

The tensile stress in the machine direction at the freeze line, S_{11F}, is given by[6,28]

$$S_{11F} = F_Z/2\pi AH \tag{1}$$

in which A and H are the radius of the tubular bubble and the film thickness, respectively, at the freeze line, and F_Z is the tensile force at the freeze line (Z),

as calculated by the following expression:

$$F_Z = F_L - 2\pi AH\rho_s g(L - Z) \tag{2}$$

where F_L is the axial tension measured at a distance L above the die exit, ρ_s is the density of the *solidified* film, and g is the gravitational acceleration. The tensile stress in the transverse direction at the freeze line, S_{33F}, is given by[6,28]

$$S_{33F} = A\Delta p/H \tag{3}$$

where Δp is the pressure inside the tubular bubble (atm) above ambient.

From a consideration of the conservation of mass we have

$$\dot{m} = \pi(a_o^2 - a_i^2)v_o\rho_m = 2\pi\rho_s AHV \tag{4}$$

where ρ_m is the density of the polymer in the *molten* state, v_o is the linear average velocity of the melt at the die exit, V is the linear velocity of the tubular bubble at the freeze line (i.e., takeup speed), and a_o and a_i are the outer and inner radius, respectively, of the die opening.

Let us now define two dimensionless parameters, blowup ratio (BUR) and takeup ratio (TUR), by

$$\text{BUR} = A/a_o \tag{5}$$

and

$$\text{TUR} = V/v_o \tag{6}$$

Substitution of eqs. (5) and (6) into eq. (4) gives

$$H = \frac{(a_o^2 - a_i^2)}{2a_o}\left(\frac{\rho_m}{\rho_s}\right)\frac{1}{(\text{BUR})(\text{TUR})} \tag{7}$$

It is of interest to note in eq. (7) that, for a given die gap opening and a given polymer, the film thickness H is inversely proportional to the product of BUR and TUR. Indeed, our experimental data support this relationship, as shown in Figure 7. Note that, in preparing the plot given in Figure 7, we measured the thickness of the film samples that were collected under a variety of processing conditions.

Substituting eq. (7) into eq. (1), with the aid of eq. (2), we obtain

$$S_{11F} = \frac{F_L}{C}\left(\frac{\rho_s}{\rho_m}\right)(\text{TUR}) - \rho_s g(L - Z) \tag{8}$$

where $C = \pi(a_o^2 - a_i^2)$. Substituting eq. (7) into eq. (3), we obtain

$$S_{33F} = \frac{1}{B}\left(\frac{\rho_s}{\rho_m}\right)(\Delta p)(\text{BUR})^2(\text{TUR}) \tag{9}$$

where $B = (a_o^2 - a_i^2)/2a_o^2$. It is now seen that the tensile stresses S_{11F} and S_{33F} in both the machine and transverse directions at the freeze line, can be calculated from measured values of axial tension F_L, takeup speed (hence TUR), bubble diameter (hence BUR), pressure inside the tubular bubble Δp, and freeze-line height Z. The striking feature of eqs. (8) and (9) is that measurements of film thickness are not needed in order to determine the tensile stresses in the tubular film at the freeze line.

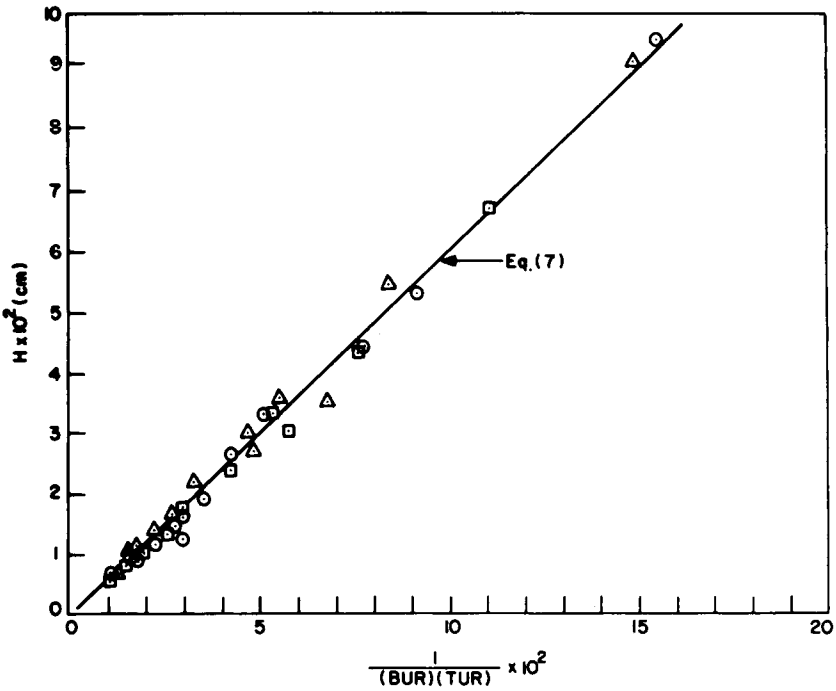

Fig. 7. Film thickness vs. the inverse of the product of blowup ratio and takeup ratio: (⊙) resin A; (△) resin B; (⊡) resin C.

RESULTS

We have calculated S_{11F} and S_{33F} at the various processing conditions employed in our experiments, using eqs. (8) and (9). Figure 8 gives plots of S_{11F} and S_{33F} vs. the blowup ratio (BUR) at various values of takeup ratio (TUR) for LDPE-A. Figures 9 and 10 give similar plots for LDPE-B and LDPE-C, respectively. A close examination of Figures 8–10 reveals, however, that the three resins give rise to, under identical processing conditions, different values of S_{11F} and S_{33F}. This is attributable to the subtle differences in their molecular characteristics (see Table I). It is seen in Figures 8–10 that, at a fixed TUR, S_{33F} increases much faster with BUR than S_{11F} does. This experimental observation can be explained with the theoretical predictions, represented by eqs. (8) and (9). Note that F_L in eq. (8) increases with BUR and, thus, S_{11F} increases with BUR.

Figure 11 gives plots of S_{11F} and S_{33F} vs. TUR at a fixed value of BUR, for the three resins investigated. It is seen that both S_{11F} and S_{33F} increase with TUR at about the same rate. This experimental observation also is readily explainable with eqs. (8) and (9).

It should be pointed out that, in film blowing operations, as TUR is increased, BUR is decreased, unless one increases Δp. Hence the experimental data obtained at different values of TUR, given in Figure 11, were obtained for different values of Δp. Note further that the axial tension F_L and the freeze-line height Z also vary with BUR and TUR.

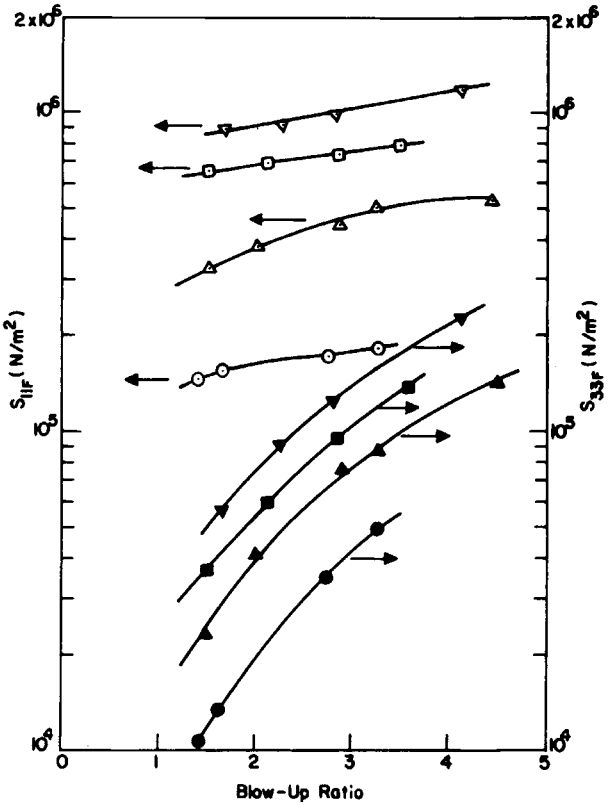

Fig. 8. S_{11F} and S_{33F} vs. blowup ratio for resin A at various takeup ratios: (⊙, ●) 3.98; (△, ▲) 9.86; (⊡, ■) 15.61; (▽, ▼) 21.44. Other processing conditions are: melt temperature 200°C; cooling air flow rate 2210 cm^3/s.

The calculation of the tensile stresses at the freeze line (see Figs. 8–11) does not shed much light on the *ultimate* film blowing characteristics of polymers. Therefore, during our experiment, we increased the takeup speed slowly until the tubular bubble broke, while maintaining the BUR and other processing conditions constant. In this way, we could determine the maximum TUR at which the tubular bubble breaks, i.e., when cohesive failure occurs. We observed that the bubble always broke in the zone below the freeze line. In other words, cohesive failure occurred when the tension applied exceeded the *ultimate* melt strength.

Figure 12 gives plots of maximum TUR vs. the cooling air flow rate at a fixed value of BUR, for the three resins investigated. It is of interest to observe that the maximum value of TUR decreases with increasing cooling air flow rate, i.e., as the tubular bubble cools faster.

In film blowing operations, one is interested in knowing the *ultimate* film thickness. Frequently one is inclined to select a grade of resin that can give rise to thin gauge films. This is understandable because, for a given amount of resin, the thinner the film, the greater area it can cover and hence the greater the profitability will be. In the tubular film producing industry one often introduces the term, "draw-down ratio (DDR)," defined as the ratio of die opening to film

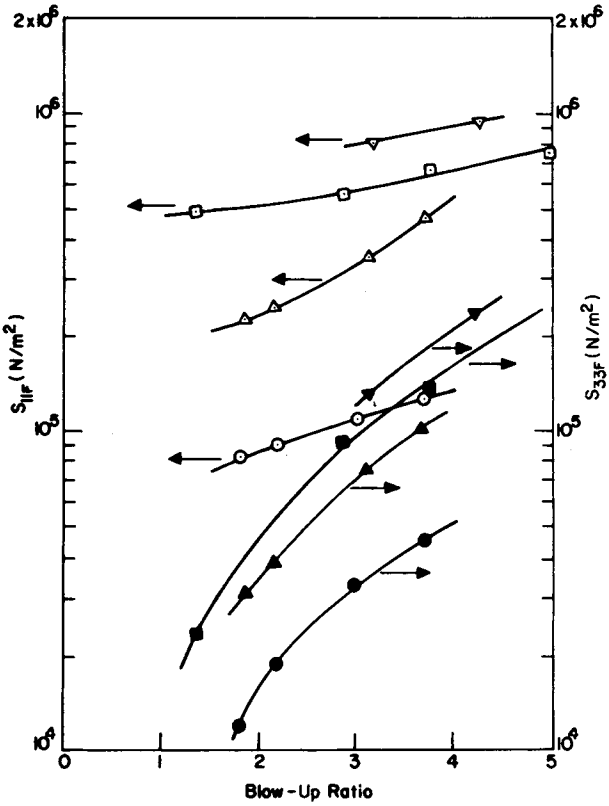

Fig. 9. S_{11F} and S_{33F} vs. blowup ratio for resin B at various takeup ratios. Symbols and other processing conditions are the same as in Figure 8.

thickness, i.e.,

$$\text{DDR} = (a_o - a_i)/H \tag{10}$$

After all, the ultimate film thickness produced depends, among many things, on the die gap opening, blowup ratio, and cooling rate. Substitution of eq. (10) into eq. (7) yields

$$\text{DDR} = \left(\frac{2a_o}{a_o + a_i}\right)\left(\frac{\rho_m}{\rho_s}\right)(\text{BUR})(\text{TUR}) \tag{11}$$

Therefore, one can now calculate the maximum DDR using eq. (11), once information on the maximum TUR at a fixed BUR is available. We have done this using the information given in Figure 12, with the aid of eq. (11), and the results are given in Figure 13.

DISCUSSION

Rheological Interpretation of Tubular Film Blowability

In reference to Figure 13, over the range of cooling air flow rate employed, the maximum DDR of the resins studied follows the sequence:

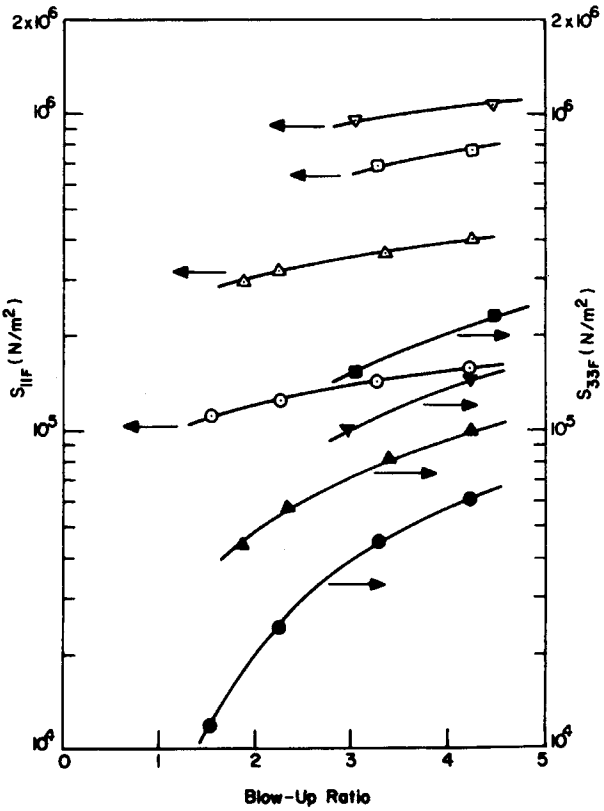

Fig. 10. S_{11F} and S_{33F} vs. blowup ratio for resin C at various take-up ratios. Symbols and other processing conditions are the same as in Figure 8.

$$\text{LDPE-C} > \text{LDPE-B} > \text{LDPE-A}$$

If we regard the maximum DDR as a measure of tubular film blowability, we can conclude that, of the three resins employed, resin C has the best blowability. We shall now attempt to interpret the experimentally observed tubular film blowing characteristics of the HP-LDPE's employed, in terms of the independently determined rheological properties of the resins.

First, the following observations may be made from Figure 2:

(i) At low shear rates,

$$\eta_A > \eta_B > \eta_C$$

(ii) At high shear rates,

$$\eta_A < \eta_B < \eta_C$$

In other words, the ordering of the shear viscosities of the three HP-LDPE's investigated are reversed as shear rate is increased from low to high values. To be specific, it appears from Table I that, at low shear rates, η depends more on the weight-average molecular weight $\overline{M}_w$ and, at high shear rates, η depends more on the number-average molecular weight $\overline{M}_n$.

It is also seen in Figure 2 that, over the entire range of shear rates investigated,

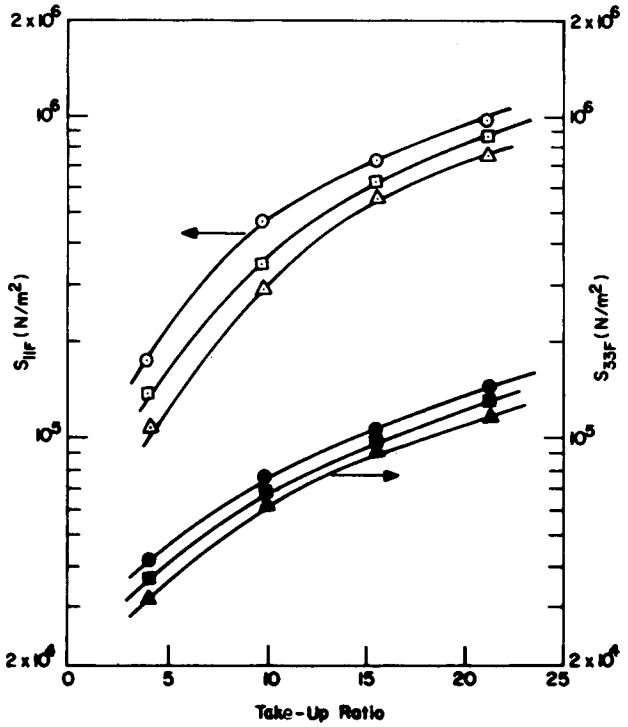

Fig. 11. S_{11F} and S_{33F} vs. takeup ratio at a blowup ratio of 3, for three LDPE's: (⊙, ●) resin A; (▲, ▲) resin B; (⊡, ■) resin C. Other processing conditions are the same as in Figure 8.

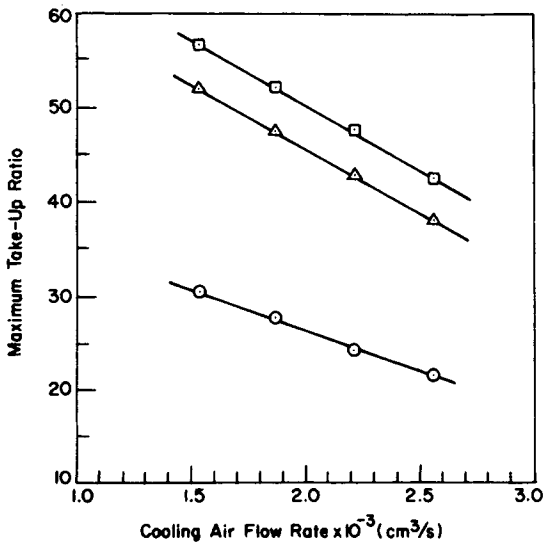

Fig. 12. Maximum takeup ratio vs. cooling air flow rate at a blowup ratio of 3.5, for three LDPE's: (⊙) resin A; (▲) resin B; (⊡) resin C. Melt temperature is 200°C.

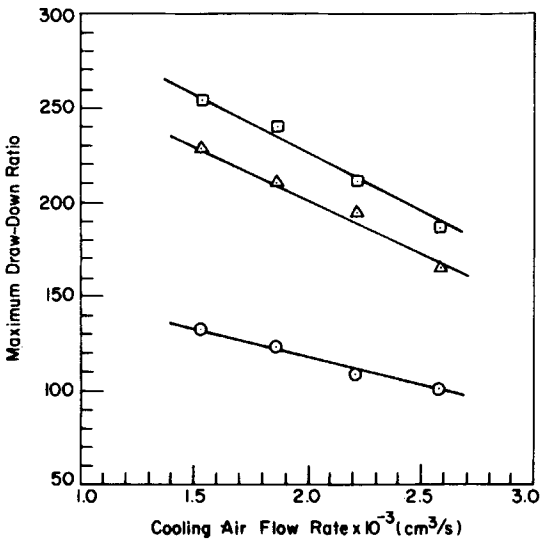

Fig. 13. Maximum draw-down ratio vs. cooling air flow rate at a blowup ratio of 3.5, for three LDPE's: (⊙) resin A; (△) resin B; (⊡) resin C. Melt temperature is 200°C.

the $\tau_{11} - \tau_{22}$ of LDPE-A is the greatest of the three resins employed, i.e.,

$$(\tau_{11} - \tau_{22})_A > (\tau_{11} - \tau_{22})_B > (\tau_{11} - \tau_{22})_C$$

There are two ways of interpreting this observation: One is that the weight-average molecular weight ($\overline{M}_w$) may control the melt elasticity, and the other is that the molecular weight distribution (MWD) may control it. Note that Table I indicates the following ordering:

$$(\text{MWD})_A > (\text{MWD})_B > (\text{MWD})_C$$

Another important molecular parameter in high-pressure low-density polyethylene (HP-LDPE) is the degree of long-chain branching (LCB). This parameter is represented by $\overline{\lambda}_n$ in Table I. Note that the larger the value of $\overline{\lambda}_n$, the greater the extent of LCB. Here $\overline{\lambda}_n$ is defined by the number of branch points per 1000 carbon atoms. It is seen in Table I that $\overline{\lambda}_n$ appears to be associated with the breadth of MWD; that is, of the three resins, LDPE-A (having the greatest amount of $\overline{\lambda}_n$) has the broadest MWD, and LDPE-C (having the least amount of $\overline{\lambda}_n$) has the narrowest MWD. Similar results were observed by Foster et al.[14] It can be concluded, therefore, from Figure 2 and Table I that the higher LCB a resin has, the more elastic the resin is.

At this juncture, it should be pointed out, in reference to Figure 2, that cone-and-plate rheometric data are of little value in understanding the rheological behavior of resins at higher shear rates, especially when the viscosity curves cross over as shear rate increases. Note that, in processing these resins, for instance, in tubular film blowing operations, the shear rates applied in the extrusion die lie in the range of 100–1000 s^{-1}. Therefore, for understanding the rheological behavior of molten polymers in the range of shear rates of practical interest, only capillary/slit rheometer data serve a useful purpose. The purpose of having included low shear-rate data in Figure 2 was to demonstrate an instance where

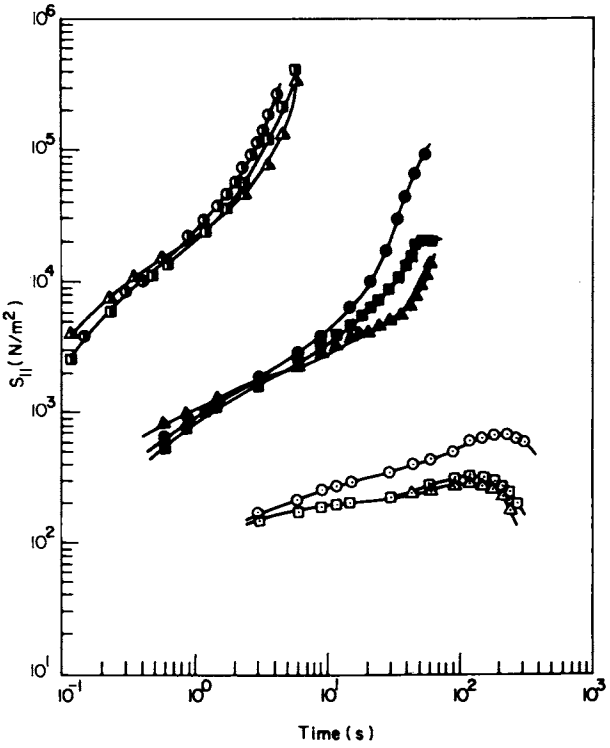

Fig. 14. Tensile stress vs. time in uniaxial elongational flow at 180°C. (a) Resin A at various values of constant elongation rate (s^{-1}): (⊙) 0.01; (●) 0.10; (◑) 1.00. (b) Resin B at various values of constant elongation rate (s^{-1}): (△) 0.01; (▲) 0.10; (◭) 1.00. (c) Resin C at various values of constant elongation rate (s^{-1}): (⊡) 0.01; (■) 0.10; (◨) 1.00.

use of low shear-rate data can lead one to draw wrong conclusions in predicting the processibility of resins.

If we now refer to the molecular parameters of the three resins employed (see Table I), the ordering of the maximum DDR, as observed in Figure 13, is correlatable to the molecular weight distribution (MWD) and the degree of long-chain branching (LCB). In other words, one can conclude that the resin having a narrower MWD and lower LCB has better tubular film blowability than the resin having a broad MWD and higher LCB.

Although, in the past, the dependency of shear flow properties on molecular parameters has been much studied, relatively little literature has been published dealing with the dependency of elongational viscosity on the molecular parameters. It appears that, in the molecular processes involved with stretching, information on elongational viscosity is at least as important as information on shear flow properties, in understanding the processability of polymeric materials.

Figure 14 describes an increase in tensile stress S_{11} as a function of time, when the specimens were subjected to a uniaxial elongation flow. It is seen that resin A has the highest rate of increase in S_{11}. In reference to Figures 3–5, for a given elongation rate, of the three resins employed, resin A has the highest elongational viscosity. With the aid of Table I, we can make the following observations on

the elongational behavior of the three resins employed. The resin having a narrow MWD and a small amount of LCB (i.e., resin C) is less *strain-hardening* (i.e., less extensional-thickening) than the resin having a broad MWD and a large amount of LCB (i.e., resin A). Since resin C has a better tubular film blowability (i.e., greater value of maximum takeup ratio and maximum draw-down ratio) than resin A, as seen in Figures 12 and 13, one can conclude that the less strain-hardening a resin is, the better the tubular film blowability will be. In other words, the strain-rate dependency of elongational viscosity is correlatable to the tubular film blowability of resin. This observation is consistent with that reported earlier by Han and co-workers,[29,30] who investigated the spinnability of various thermoplastic resins in melt spinning operations.

According to Minoshima et al.[31] the elongational viscosity of narrow MWD samples of polypropylene increases with increasing elongation rate, whereas the elongational viscosity of broad MWD samples decreases with increasing elongation rate, over the range of elongation rates, 0.01–1.0 s^{-1}, tested. They report further that the elongation to break (equivalent to the maximum draw-down ratio) of the narrower MWD samples is greater than that of the broader MWD samples, and increases with decreasing molecular weight. By conducting isothermal melt spinning experiments, Minoshima et al.[32] observed that the *apparent* elongational viscosity of the broad MWD samples of polypropylene decreases rapidly with increasing elongation rate, whereas the narrow MWD samples have constant or mildly decreasing *apparent* elongational viscosities.

From the practical point of view, it is highly desirable to have a criterion (or criteria) for the choice of resins that will give good tubular film blowability, without having to perform a time-consuming tubular film blowing operation. Such a criterion, once established, will help the resin producers to tailor-make specific resins for certain applications and, also, will help the tubular film producers to conduct routine tests of the quality of the resin that they receive from the resin producers.

Based on the experimental results presented above, we conclude from the molecular point of view that the resin having a narrow MWD and low degree of LCB has better tubular film blowability than the resin having a broad MWD and high degree of LCB. On the other hand, we conclude from the rheological point of view that a resin having lower melt elasticity in shearing flow and exhibiting less strain-hardening behavior in elongational flow tends to give a greater draw-down ratio, indicating a better tubular film blowability.

Optical Properties of the Tubular Blown Films

From the end-use point of view, the clarity of film is very important for certain applications. Table II summarizes typical measurements of the gloss and haze of the tubular blown films produced in our experiment. It is seen that, of the three resins investigated, resin C has the highest value of gloss and the lowest value of haze.

Earlier, Huck and Clegg[33] pointed out that the haze (or gloss) of tubular blown films depends very much on the surface irregularities and the size of crystalline domain in the films, which in turn are dependent upon the processing conditions employed. Since, in our study, the films were produced under essentially identical processing conditions, we can conclude that the observed differences

TABLE II
Gloss and Haze of the Tubular Blown Films Produced[a]

Resin	45° specular gloss	Haze (%)	BUR	TUR
A	53.3	9.9	3.2	4.0
B	73.5	8.4	3.0	4.0
C	75.2	6.5	3.2	4.0

[a] Melt extrusion temperature = 200°C; cooling air flow rate = 2210 cm^3/s.

in the haze and gloss of the tubular blown films (see Table II) may be attributable to the differences in the degree of LCB of the three resins investigated. A clear trend is seen in Table II that the haze increases (and the gloss decreases) as the degree of LCB increases (see, also, Table I). A similar observation was reported by Foster et al.[14] However, further investigation is needed for determining how much the degree of LCB influences the surface irregularities and the crystallization behavior of HP-LDPE during the cooling of tubular blown bubble.

Tensile Properties of the Tubular Blown Films

One would expect that processing conditions affect the mechanical properties of the tubular blown films. Table III summarizes typical test results of ultimate tensile strength for the tubular blown films obtained at various values of BUR

TABLE III
Ultimate Tensile Strength of the Tubular Blown Films Produced

BUR	TUR	MD (MPa)	TD (MPa)
		(a) Resin A	
1.4	3.9	14.28	12.49
1.6	3.9	14.28	13.05
2.7	3.9	13.99	13.95
3.2	3.9	14.66	15.46
2.9	9.8	17.20	13.10
2.9	15.6	22.60	12.10
2.8	21.4	24.68	9.50
		(b) Resin B	
1.7	3.9	13.62	13.49
2.2	3.9	13.99	14.12
3.0	3.9	13.96	14.59
3.7	3.9	13.83	15.90
3.1	9.8	15.98	12.90
2.9	15.6	21.50	12.10
3.1	21.4	24.80	11.20
		(c) Resin C	
1.5	3.9	14.43	14.08
2.2	3.9	14.05	15.18
3.2	3.9	14.71	15.34
4.2	3.9	14.49	16.29
3.4	9.8	16.06	15.10
3.3	15.6	21.80	13.20
3.0	21.4	24.72	10.85

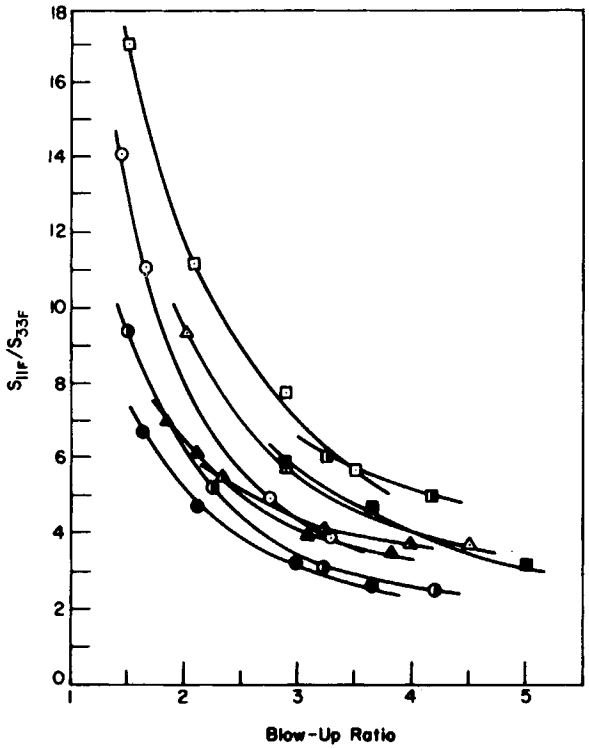

Fig. 15. S_{11F}/S_{33F} ratio vs. blowup ratio for the three LDPE's employed. (a) Resin A at various takeup ratios: (⊙) 4.4; (▲) 9.9; (⊡) 15.6. (b) Resin B at various takeup ratios: (●) 4.4; (▲) 9.9; (■) 15.6. (c) Resin C at various takeup ratios: (◑) 4.4; (▲) 9.9; (◨) 15.6. Other processing conditions are the same as in Figure 8.

and TUR. The following observations may be made on the results given in Table III: (1) at a fixed TUR, an increase in BUR increases the transverse direction (TD) tensile strength, but has little influence on the machine direction (MD) tensile strength; (2) at a fixed BUR, an increase in TUR increases the MD tensile strength and decreases the TD tensile strength. It should be pointed out, however, that, during the tensile strength test, we observed the occurrence of necking in the test specimens. Therefore, the results given in Table III must not be construed as the sole consequence of processing conditions employed. In the present investigation, we could not observe any discernible difference in the ultimate tensile strength of the films that were obtained with three different grades of LDPE at comparable processing conditions. Therefore, we cannot comment on the effect of the degree of LCB on film strength.

We are also interested in the tensile strength of the *as-blown* tubular film. If we assume that there is no molecular orientation occurring in the tubular blown bubble above the freeze line, the values of S_{11F} and S_{33F}, which may be calculated from eqs. (8) and (9), respectively, represent the MD and TD tensile strength, respectively, of the *as-blown* tubular films. In order to facilitate our discussion here, plots of S_{11F}/S_{33F} ratio vs. blowup ratio are given in Figure 15, with the takeup ratio as parameter. It is seen that the S_{11F}/S_{33F} ratio decreases with BUR, and increases with TUR, and that resin A (having a broad MWD) exhibits

higher values of S_{11F}/S_{33F} ratio than the other two resins, over the range of TUR and BUR investigated. Note that, with the aid of eqs. (8) and (9), the S_{11F}/S_{33F} ratio can be represented by

$$\frac{S_{11F}}{S_{33F}} = \left[\frac{F_L}{2\pi a_o^2 \Delta p} - \frac{B\rho_m g(L-Z)}{(\Delta p)(\mathrm{TUR})}\right]\frac{1}{(\mathrm{BUR})^2} \tag{12}$$

It is of interest to note in eq. (12) that we can make the tensile property *isotropic* (i.e., $S_{11F} = S_{33F}$) by judiciously changing the processing variables (i.e., Δp, TUR, and BUR) and the die design variables, (i.e., die gap opening, $a_o - a_i$, and die radius, a_o).

It is worth mentioning at this juncture that the applied stresses, S_{11F} and S_{33F}, are intimately related to the molecular orientations and, thus, to the mechanical anisotropy of the blown film. As a matter of fact, for amorphous polymers eq. (12) also represents the ratio of amorphous orientation factors, f_1^B/f_3^B. Note that the f_1^B/f_3^B ratio is dependent upon both the processing variables and die design variables. However, at present there exists no theory that relates the crystalline orientation factors to the applied stresses for semicrystalline polymers, such as the low-density polyethylenes investigated in the present study. This is a subject which requires further investigation.

We wish to express our gratitude to the following individuals, without whose help the study reported here would not have been possible. Dr. George N. Foster at Union Carbide Corp. has supplied us not only with the resins, but also with their molecular characteristics, as reported in Table I; Mr. Yong Joo Kim measured the high-shear flow properties, and Mr. Hsiao-Ken Chuang measured the low-shear flow properties, of the resins, as reported in Figure 2; Professor James L. White at the University of Tennessee allowed us to use the elongational rheometer in his laboratory.

References

1. E. B. Bagley, *J. Appl. Phys.*, **31,** 1126 (1960).
2. J. E. Guillet, R. L. Combs, D. F. Slonaker, D. A. Weems, and H. W. Coover, *J. Appl. Polym. Sci.*, **9,** 757, 767 (1965).
3. R. L. Combs, D. F. Slonaker, and H. Coover, *J. Appl. Polym. Sci.*, **13,** 519 (1969).
4. L. Wild, R. Ranganath, and D. C. Knobeloch, *Polym. Eng. Sci.*, **16,** 811 (1976).
5. C. D. Han and C. A. Villamizar, *J. Appl. Polym. Sci.*, **22,** 1677 (1978).
6. C. D. Han, *Rheology in Polymer Processing*, Academic, New York, 1976.
7. Z. Grubisic, P. Remp, and H. Benoit, *J. Polym. Sci.*, **B5,** 753 (1967).
8. A. E. Hamielec and A. C. Ouano, *J. Liq. Chromatgr.*, **1,** 111 (1978).
9. E. E. Drott and R. A. Mendelson, *J. Polym. Sci., A-2*, **8,** 1373 (1970).
10. A. Ram and J. Miltz, *J. Appl. Polym. Sci.*, **15,** 2639 (1971).
11. A. C. Ouano and W. Kaye, *J. Polym. Sci., A-1*, **12,** 1151 (1974).
12. A. C. Ouano, *J. Chromatogr.*, **118,** 303 (1976).
13. T. B. MacRury and M. L. McConnell, *J. Appl. Polym. Sci.*, **24,** 651 (1979).
14. G. N. Foster, A. E. Hamielec, and T. B. MacRury, ACS Symposium Series, No. 138, American Chemical Society, Washington, D.C., 1980, p. 131.
15. R. Farber and J. M. Dealy, *Polym. Eng. Sci.*, **14,** 435 (1974).
16. C. D. Han and J. Y. Park, *J. Appl. Polym. Sci.*, **19,** 3257 (1975).
17. C. D. Han and J. Y. Park, *J. Appl. Polym. Sci.*, **19,** 3277 (1975).
18. C. D. Han and J. Y. Park, *J. Appl. Polym. Sci.*, **19,** 3291 (1975).
19. C. D. Han and R. Shetty, *Ind. Eng. Chem. Fundam.*, **16,** 49 (1977).
20. W. F. Maddams and J. E. Preedy, *J. Appl. Polym. Sci.*, **22,** 2721 (1978).
21. W. F. Maddams and J. E. Preedy, *J. Appl. Polym. Sci.*, **22,** 2739 (1978).
22. W. F. Maddams and J. E. Preedy, *J. Appl. Polym. Sci.*, **22,** 2751 (1978).
23. W. F. Maddams and J. E. Preedy, *J. Appl. Polym. Sci.*, **22,** 3027 (1978).

24. K. J. Choi, J. E. Spruiell, and J. L. White, *J. Polym. Sci., Polym. Phys. Ed.*, **20,** 27 (1982).
25. K. J. Choi, J. L. White, and J. E. Spruiell, *J. Appl. Polym. Sci.*, **25,** 2777 (1980).
26. K. Matsumoto, J. F. Fellers, and J. L. White, *J. Appl. Polym. Sci.*, **26,** 85 (1981).
27. Y. Ide and J. L. White, *J. Appl. Polym. Sci.*, **22,** 1061 (1978).
28. J. R. A. Pearson and C. J. S. Petrie, *J. Fluid Mech.*, **40,** 1 (1970).
29. C. D. Han and R. R. Lamonte, *Trans. Soc. Rheol.*, **16,** 447 (1972).
30. C. D. Han and Y. W. Kim, *J. Appl. Polym. Sci.*, **18,** 2589 (1974).
31. W. Minoshima, J. L. White, and J. E. Spruiell, *Polym. Eng. Sci.*, **20,** 1166 (1980).
32. W. Minoshima, J. L. White, and J. E. Spruiell, *J. Appl. Polym. Sci.*, **25,** 287 (1980).
33. N. D. Huck and P. L. Clegg, *Soc. Plast. Eng. Trans.* **1**(3), 121 (1961).

Received November 9, 1982
Accepted June 1, 1983